Mutual Inductance Evaluation Between Two Parallel Conductors on a PCB

Sana Chouaibi
CES Laboratory, National engineering school of Sfax (ENIS), Sfax University, Tunisia
National Engineering School of Sousse (ENISo), Sousse University, Tunisia
sana.chouaibi@eniso.u-sousse.tn

Mohamed Hadj Said
Center for Research in Microelectronics & Nanotechnology (CRMN), Sousse, Tunisia
SI2E Laboratory, National Engineering School of Sfax, Sfax University,Tunisia
mohamed.hadjsaid@crmn.rnrt.tn

Dorra Nasr
Center for Research in Microelectronics & Nanotechnology (CRMN), Sousse, Tunisia
Laboratory of Microelectronics and Instrumentations, Faculty of Sciences of Monastir, Tunisia
dorra.nasr@isimm.u-monastir.tn

Mossaad Ben Ayed
CES Laboratory, National Engineering School of Sfax (ENIS), Sfax University, Tunisia
National Engineering School of Sousse (ENISo), Sousse University, Tunisia
mossaad.benayed@eniso.u-sousse.tn

Denis Flandre
SMALL Research Group, ICTEAM Institute, Université catholique de Louvain, Belgium
denis.flandre@uclouvain.be

Fares Tounsi
SMALL Research Group, ICTEAM Institute, Université catholique de Louvain, Belgium
SI2E Laboratory, National Engineering School of Sfax, Sfax University,Tunisia
fares.tounsi@uclouvain.be

2023 30th IEEE International Conference on Electronics, Circuits and Systems (ICECS) | 979-8-3503-2649-9/23/$31.00 ©2023 IEEE | DOI: 10.1109/ICECS58634.2023.10382803

***Abstract*—In this paper, we present a comprehensive analysis of two parallel conductors, fabricated on a printed circuit board (PCB), forming an elementary planar transformer, with an emphasis on extracting performance parameters such as self-inductance, resistance, coupling coefficient, mutual inductance, and inter-winding capacitance. Results issued from theoretical equations, FEM-based simulations, and characterizations were compared together to evaluate the mutual inductance. A procedure using the Open-Short de-embedding technique has been successfully applied to extract the correct performance values.**

Keywords—Planar transformer, mutual inductance, coupling coefficient, de-embedding method, parallel conductors.

I. INTRODUCTION

Printed circuit board (PCB)-based planar transformers offer several advantages over standard wire-wound transformers, such as miniature dimensions, good thermal properties, high power density, simplicity of manufacture, low cost, and high reliability [1][2]. The operating principle of the transformer is based on the mutual induction coupling of two or more conductors (or windings). It is designed to couple alternating currents from one winding to another (DC current flow is inhibited by the transformer) in such a way as to avoid a large loss of power [3]. In the operation of transformers, mutual inductance is an essential criterion in inductive circuits, as it describes the power transfer capability. Thus, when designing transformers, it is desirable to achieve a high level of mutual inductance to ensure efficient energy transmission. Numerous studies in the literature focus on improving this factor, often by incorporating magnetic materials into transformer design. Acero *et al.* [4] succeeded in significantly improving mutual inductance by a factor of 4 by introducing non-conducting magnetic plates. The addition of magnetic materials increases the coupling between windings, which in turn improves the transformer's performance.

Planar transformers can be classified mainly into three different topologies depending on their implementation, namely: stacked, interleaved, and tapped. In a stacked transformer (or Finlay), primary and secondary coils are implemented in two different superimposed metal layers [5]. For the interleaved transformer (or Frlan), both windings are sketched symmetrically on the same plane, so mutual inductance is lower than that of the stacked device [6]. Tapped transformer, or concentric transformer, is the less examined topology wherein both wound planar spirals are implemented concentrically in the same top metal layer [7]. Each structure meets specific needs: stacked transformers improve performance, especially in terms of magnetic coupling (due to their tight geometry) and inductance leakage; interleaved transformers are considered to be more symmetrical, but they generally have lower mutual inductance; and tapped transformers offer better self-inductance and reduced winding capacity but suffer from a weak coupling coefficient [8]. Planar transformers are preferred in certain applications where compactness and high-frequency operation are essential [5]. They are commonly employed in RF and communication systems to adapt impedance and convert differential signals into unbalanced ones [9]. In these applications, it is necessary to emphasize the importance of calculating and improving the coupling coefficient (or mutual inductance), especially since many systems rely on inductive coupling as a fundamental operating principle.

Since parallel conductors form the basis of planar transformers, a study of this basic configuration is essential to facilitate a clear understanding and, thus, the ability to evaluate the mutual inductance between the windings of a planar transformer. Prominent approaches in this endeavor include methodologies introduced by Greenhouse, Biot-Savart, etc. [10] However, research on mutual inductance between planar sets of conductors remains incomplete, and research is underway in the literature to discover more accurate methods for its calculation. Hence, this article deals with the physical analysis of a planar elementary transformer based on two parallel conductors, with the aim of studying and validating the theoretical model through simulation and practical measurement set-up and procedures to mainly evaluate the coupling coefficient and the mutual inductance. This paper is organized as follows: Section II focuses on the theoretical background. The design, fabrication, and modeling of the proposed transformer are discussed in Section III. FEM-based simulations and characterizations are presented in Section IV, and Section V is devoted to the conclusion.

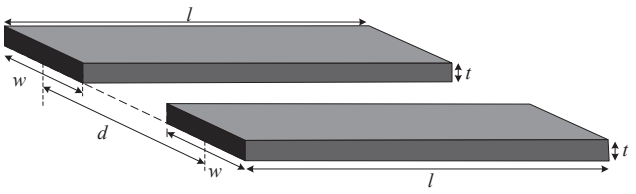

Fig. 1. A parallel arrangement of two equal-length conductors.

II. THEORETICAL EVALUATION

A wire of any length features some self-inductance. For most applications, this self-inductance is ignored because it is too low to have any significant effect on the circuit. However, as frequencies rise towards the microwave region (>300 MHz), even the inductance of short lengths of wire can have a significant effect. The self-inductance expression of a rectangular conductor was given by Grover as [11]:

$$L_{DC} = \frac{\mu_0 l}{2\pi}\left[ln\left(\frac{2l}{w+t}\right) + 0.5 + \frac{2(w+t)}{9l}\right] \quad (1)$$

where w, t, and l represent the width, thickness, and length of the conductor, respectively, and μ_0 is the permeability of free space (Fig. 1). This expression is valid as long as the width or thickness of the conductor is not twice its length, as in typical designs. Besides, when two conductors are placed a short distance apart, as shown in Fig. 1, and a current flows through one of them, this gives rise to a transformer. The mutual inductance between these two conductors mainly depends on their intersection angles, length, and separation distance. For instance, two orthogonal conductors do not have mutual inductance because their magnetic fluxes are not coupled to each other. In the simple case of two parallel conductors of the same length l and rectangular section of width w and thickness t (Fig. 1), placed next to each other at a distance separating their centers equal to d, the mutual inductance between them is defined by [11]:

$$M = \frac{\mu_0 l}{2\pi} Q \quad (2)$$

where Q is a coefficient that depends only on the geometry and is given by [11]:

$$Q = \left[ln\left(\sqrt{1+\frac{l^2}{GMD^2}} + \frac{l}{GMD}\right) - \sqrt{1+\frac{GMD^2}{l^2}} + \frac{GMD}{l}\right] \quad (3)$$

where GMD is the geometric mean of the distance between the surfaces of two conductors. In the case of two parallel rectangular conductors (Fig. 1), the exact value of the GMD can be estimated with an error of less than 3% by [11]:

$$ln(GMD) = ln(d) - \left\{\frac{w^2}{12d^2} + \frac{w^4}{60d^4} + \frac{w^6}{168d^6} + \frac{w^8}{360d^2} + \frac{w^{10}}{660d^{10}} + \cdots\right\} \quad (4)$$

As expected, the GMD is slightly smaller than the distance d between the two conductor centers. The mutual inductance varies slightly relative to the width of the conductor when the distance between the two centers remains fixed. This implies that the value of the mutual inductance between two inductors with similar distances between spirals barely changes when the width of these spirals is modified.

III. THE TRANSFORMER FABRICATION AND BACKGROUND

In order to evaluate the self- and mutual inductances between two conductors, these have been printed as tracks on an FR4-based PCB to provide structural support, precise geometric definition, and a ground plane surrounding the structure. The use of FR-4 (fiberglass and epoxy resin) as a substrate, easily accessible, makes the structure lightweight, quick to produce, and inexpensive to manufacture. Fig. 2 shows the 3D schematic of the two straight parallel conductors (in the center), forming a basic planar transformer, with their feeding tracks to the two input/output ports and the ground plane. A small gap is investigated to obtain a fairly detectable inductive coupling. All planar structures (parallel conductors and de-embedding fixtures) were patterned on a double-sided PCB (17 µm copper thickness and 1.7 10^{-8} Ω·m as resistivity) with a minimal drill bit resolution equal to 400 µm. The basic transformer geometric parameters are given in TABLE I. It should be noted that the gap between the two conductors D (with $D = d - w$) has a tremendous impact on the performance of the transformer.

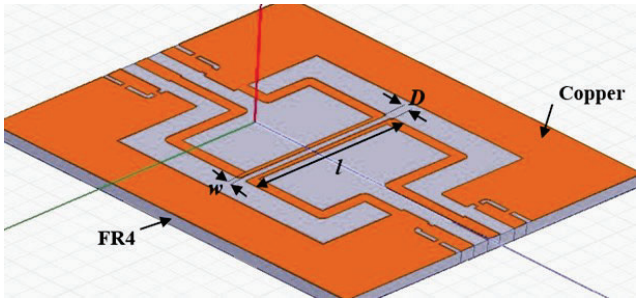

Fig. 2. 3D schematic of the PCB-based two parallel conductors (orange color is used for Cu tracks, grey for FR-4 substate).

TABLE I. TRANSFORMER PARAMETRES.

Parameter	l	w	t	D
Value (mm)	15.6	0.4	0.017	1.2

The planar transformer can be modeled with the lumped-element electrical circuit of Fig. 3, where each conductor is presented by a self-inductance (L_1 or L_2) in series with an internal resistor (R_{s1} or R_{s2}). P_1 and P_2 denote the input and output signal ports of the primary and secondary windings, respectively, and G is the ground. A mutual inductance, M, or inductive coupling, which is the principal property of transformers, exists only when two or more conductors are located such that the magnetic flux generated by one of them finds a path to connect the other adjacent conductors. In practice, a planar transformer includes several parasitic components, including stray capacitances to ground (C_{s1} and C_{s2}, modeling the capacitance between the structure and the surrounding ground plane) and inter-winding capacitance (C_i, modeling the capacitive coupling between the two parallel conductors). The combination of these two capacitances causes the transformer to self-resonate at a specific frequency, which stops the transfer of electrical energy. In this implementation, it is worth emphasizing that we have chosen to analyze the opposite series configuration (Fig. 2). The self-inductances (L_{r1} and L_{r2}) and the resistors (R_{r1} or R_{r2}) represent the remaining parts of the structure tracks that are not part of the transformer and will be removed by de-embedding.

When actuated by time-varying currents i_1 and/or i_2, the magnetic interaction between the two conductors will induce four flux components: Φ_{11}, Φ_{12}, Φ_{22}, and Φ_{21}. The

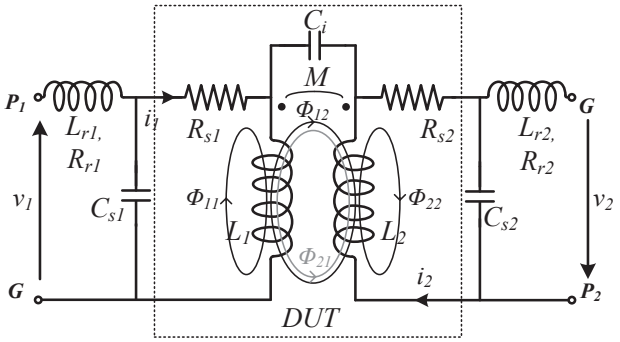

Fig. 3. The lumped element electrical model of the two parallel coupled conductors (with dot notation), including magnetic and capacitive couplings.

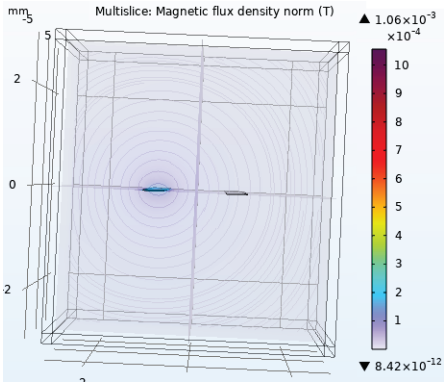

Fig. 4. Magnetic field created around the primary conductor.

current i_1 produces a magnetic flux Φ_1, part of which is lost as flux coupling, Φ_{12}, and the other part, Φ_{11}, passes through the circuit itself (and similarly for i_2) according to:

$$\begin{cases}\phi_1 = \phi_{11} + \phi_{21} = L_1 i_1 + M_{21} i_2 \\ \phi_2 = \phi_{22} + \phi_{12} = L_2 i_2 + M_{12} i_1\end{cases} \quad (5)$$

where the mutual inductance, M_{12}, is defined as the ratio between the flux generated by circuit 1 through circuit 2 (Φ_{12}) to the current flowing in circuit 1 (i_1), and analogously for M_{21}. According to Faraday's law, the change in flux generated by the magnetic field through one of the two conductors induces an electromotive force (*emf*) across the other. The *emf* mainly depends on the frequency of the current and the mutual inductance. The amount of inductive coupling between the two conductors, due to the variation in magnetic flux, is measured by their mutual inductance, which can be defined by:

$$M_{12} = k\sqrt{L_1 L_2} \quad (6)$$

where k is the magnetic coupling coefficient between the primary and secondary, which is between 0 and 1. For an ideal transformer, $k = 1$, but for most planar transformers, k is between 0.3 and 0.9 due to magnetic flux leakage. In practice, reasons for this non-ideality include the skin effect, proximity effect, eddy currents, parasitic capacitance, and resistance due to ohmic losses.

IV. Simulation and Characterization

A. FEM analysis and simulation

COMSOL Multiphysics software can be used to extract the self-inductance of each conductor and the mutual inductance of the arrangement considered. The self-inductance and the mutual inductance can be calculated using a steady-state study with the physical interface 'Magnetic Fields (mf)' under a 'stationary' analysis. The simulated values will be compared with analytical expressions to verify the accuracy of the FEM model. The modeled domain is surrounded by an aerial infinite element region, which is a way to carve out a domain that extends to infinity. Both conductors are modeled using the 'one-turn coil' function, while the primary conductor will only be excited with a DC current $I_1 = 1$ A. The DC magnetic field it creates around the primary conductor gradually varies with distance, as shown in Fig. 4, and passes through the other winding of the transformer. However, because this current is constant, the magnetic flux through the secondary will not change, meaning no voltage is induced. Despite this, self-inductance and mutual inductance could be calculated in this static analysis by evaluating the total magnetic flux across the appropriate closed surface. Self-inductance is defined as the magnetic flux B passing through the closed surface S_1, as:

$$L_{DC} = \frac{\iint_{S_1} Bn\, ds}{I_1} \quad (7)$$

where n is the vector normal to the primary conductor plan, and the integral is taken over the surface S_1 defined by the primary conductor edges. Mutual inductance is defined when replacing S_1 with S_2, the edges of which are defined by the secondary conductor.

B. Characterization and measurements

In this section, we will discuss the results of the measurements along with those from simulations. The PCB-based transformer was characterized using a Keysight E5080A ENA vector network analyzer connected via a 50 Ω SMA connector (Fig. 5a). The VNA collected data from the S-parameter scattering matrix within the frequency range of 1 MHz to 3 GHz. SOLT (Short-Open-Load-Thru) is used to calibrate the latter, allowing the reference plane to be shifted to the SMA connector terminals. To push the reference plane further toward the DUT (device under test), an additional Open-Short de-embedding procedure is necessary. Measurements of two standard structures are needed, realized using the same materials and designs of input/output ports and ground plane as the DUT: the Open, i.e., comprising all the tracks of the circuit except the two parallel conductors (Fig. 5b), and the Short, i.e., with all ports connected together to the ground (Fig. 5c). The measurement data corresponding to the two insulated parallel conductors (our DUT) can be obtained through:

$$Y_{cond} = \left[\left(Y_{DUT} - Y_{open}\right)^{-1} - \left(Y_{short} - Y_{open}\right)^{-1}\right]^{-1} \quad (8)$$

Thus, according to Eq. 8, the procedure for the Open-Short de-embedding technique can be detailed as follows:

• Measure the S-parameters (S_{DUT}, S_{open}, and S_{short}) for the DUT, open, and short structures and convert them to Y-parameters (Y_{DUT}, Y_{open}, and Y_{short});

• Perform the first step of the de-embedding by removing the parallel parasitics from both Y_{DUT} and Y_{short} according to:

$$Y_{DUT1} = Y_{DUT} - Y_{open} \quad (9)$$

$$Y_{short1} = Y_{short} - Y_{open} \quad (10)$$

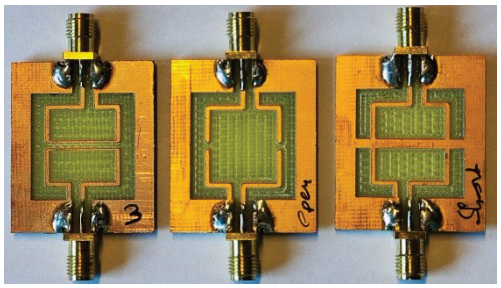

Fig. 5. The PCB-based circuits: (a) the transformer (formed by the two parallel conductors), (b) the open structure, and (c) the short structure.

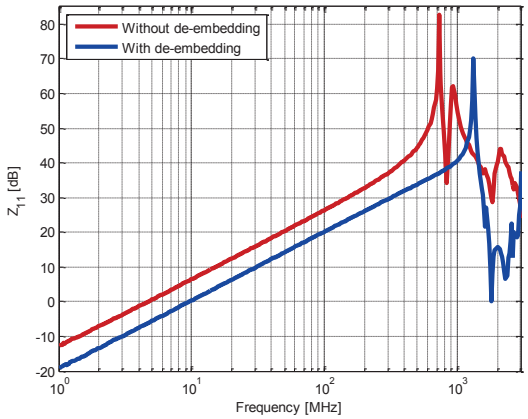

Fig. 6. Comparison between uncorrected Z_{11} data (in red) and Open-Short de-embedded Z_{11} data (in blue).

• Perform the second step of the de-embedding by removing the series parasitics Z_{short1} (converted from Y_{short1}) from Z_{DUT1} (converted from Y_{DUT1}) according to:

$$Z_{transformer} = Z_{DUT1} - Z_{short1} \tag{11}$$

Fig. 6 shows the Z_{11} measurement data before and after the three-step deembedding procedure. A significant decrease in the impedance data before and after de-embedding is observed, which is expected since we removed the contribution from tracks that are not parallel. It is worth noting that the resonance frequency on the Z_{11} increases from 730 MHz to 1330 MHz as the stray capacitances (C_{s1} and C_{s2}) are subtracted by the de-embedding. The new shifted resonance observed on Z_{11} is due to the inter-winding parasitic capacitance C_i, which creates a leak and stops the magnetic transfer of energy.

Self-inductance measurements play a crucial role in understanding the characteristics and performance of transformers. These measurements tell us about the ability of the winding to preserve magnetic energy when a current passes through it. The self-inductance evaluation for the primary conductor can be assessed using:

$$L_1 = \frac{Im(Z_{11})}{2\pi f} \tag{12}$$

Fig. 7 represents the evaluation of the inductance L_1, extracted by Eq. 12 from the measurements, which shows a value of 16.55 nH at 10 MHz after the de-embedding. The inductance of the second conductor can also be evaluated by replacing Z_{11} with Z_{22} in Eq. 12. In addition, resistance plays a role in determining the transformer's ability to conserve magnetic energy by controlling ohmic losses. The series resistance of the primary winding can be extracted by:

$$R_{s1} = Re[Z_{11}] \tag{13}$$

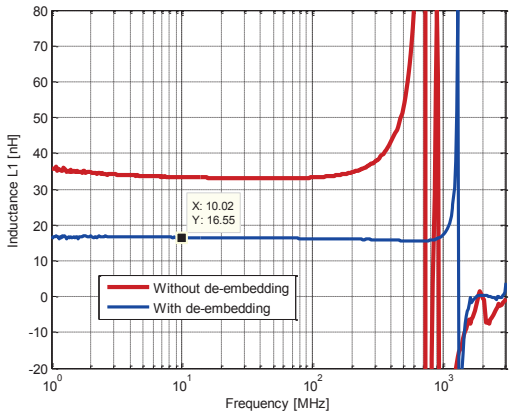

Fig. 7. Inductance evaluation of the primary conductor extracted from measurements: uncorrected data (in red) and Open-Short de-embedded data (in blue).

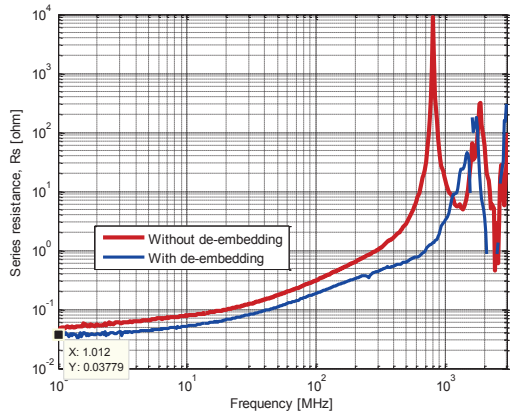

Fig. 8. Series resistance evaluation of the primary conductor extracted from measurements: uncorrected data (in red) and Open-Short de-embedded data (in blue).

Similarly, the resistance of the secondary conductor R_{s2} can also be evaluated by substituting Z_{11} with Z_{22} in Eq. 13. Fig. 8 shows the primary conductor resistance extracted from the measurements. The coupling coefficient k between the two conductors can be expressed from the Z-parameter and will be given by:

$$k = \sqrt{\frac{Im(Z_{12})\ Im(Z_{21})}{Im(z_{11})\ Im(Z_{22})}} \tag{14}$$

The coupling coefficient is represented in Fig. 9, and is found to be 0.221. Additionally, we analyze the mutual inductance between the primary and secondary windings. This amount quantifies the magnetic coupling between the two windings, which is crucial for efficient energy transfer. In other words, it indicates the degree of interaction between the primary and secondary windings. The equation to extract this parameter is [12]:

$$M = -\frac{Im(z_{12})}{2\pi f} \tag{15}$$

It should be noted that the minus sign in Eq. 15 comes from the fact that the two conductors are in indirect coupling. The mutual inductance, extracted using both Eq. 6 and Eq. 15, is plotted in Fig. 10 and is evaluated to be 3.53 nH. The main important parameters extracted from our study are presented in TABLE II. Looking at the collected results, we can see a difference of up to about ±30% between the theoretical, simulated, and measured results, especially regarding the theoretical mutual inductance, which will be addressed in depth in future works.

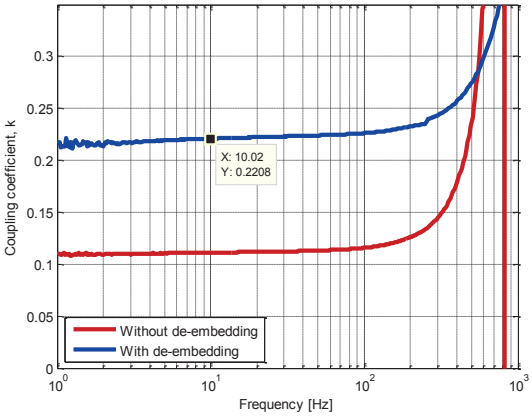

Fig. 9. Coupling coefficient between two conductors extracted from uncorrected data (in red) and Open-Short de-embedded data (in blue).

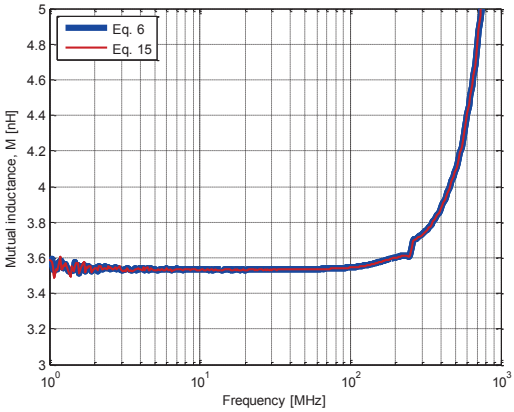

Fig. 10. Mutual inductance between the two conductors extracted from measurements after de-embedding.

TABLE II. MAIN EXTRACTED PARAMETERS.

Parameter	Measurement	Theoretical	Simulation
L₁ (nH)	16.55	15.17	13.53
M (nH)	3.53	6.45	4.72
k	0.221	0.425	0.34

Here, it is obvious that the mutual inductance is only measurable within the frequency band where the inductive coupling exists, i.e., up to 200 MHz (Fig. 10). In addition to the mutual inductance link between the two conductors, a capacitive coupling coexists. The inter-winding capacitance between primary and secondary could be evaluated from the resonant frequency of Z_{12} as:

$$C_i = \frac{1}{L_1(2\pi f)^2} \qquad (16)$$

where L_1 is the self-inductance of the primary, which gives an interwinding capacitance equal to 0.86 pF. The extracted lumped element electrical model was implemented on Advanced Design System (ADS) software to verify its conformity with the measurements and also to figure out C_{s1} and C_{s2} values. With an identical value of stray capacitances equal to 1.675 pF on both windings, the resonant frequency of the transformer is identical to that found in the curves of Z_{12} before the de-embedding (Fig. 11a), and after the de-embedding (Fig. 11b).

V. CONCLUSION

In this work, the coupling coefficient and the mutual inductance between two parallel conductors, fabricated on a

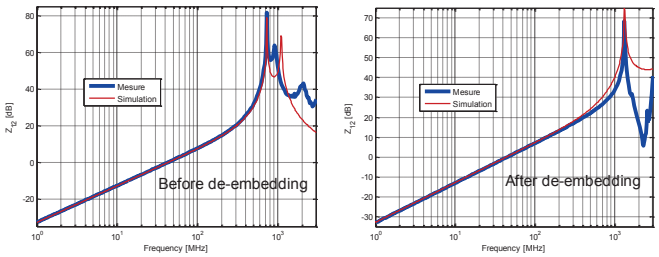

(a) (b)

Fig. 11. Comparison between the Z_{12} from the simulation of the equivalent electrical model and that measured: (a) before de-embedding, and (b) after de-embedding.

PCB, were investigated in depth. Measurement results using well-designed structures and a VNA in the 1 MHz–3 GHz frequency band show that de-embedding correction properly recovers the values of the self-inductance, mutual inductance, and coupling coefficient. These three coefficients were found to show some discrepancy of up to ±30% between the theoretical equations, COMSOL simulations, and VNA measurements to be further examined. The parasitic components, including the stray capacitance to ground and the interwinding capacitance, were also extracted, and the lumped-element electric model implemented in ADS simulation fairly reproduces the measurements. The results obtained here are of importance to establish the basic building blocks used when designing other types of more complicated planar transformers.

REFERENCES

[1] H. Shamkhalichenar, C. J. Bueche, and J.-W. Choi, "Printed Circuit Board (PCB) Technology for Electrochemical Sensors and Sensing Platforms," Biosensors, vol. 10, No. 11, pp. 159, Oct. 2020.

[2] G. K. Y. Ho, Y. Fang, and B. M. H. Pong, "A Multiphysics Design and Optimization Method for Air-Core Planar Transformers in High-Frequency LLC Resonant Converters," IEEE Trans. Ind. Electron., vol. 67, No. 2, pp. 1605-1614, Feb. 2020.

[3] J. R. Long, "Monolithic transformers for silicon RF IC design," IEEE J. Solid-State Circuits, vol. 35, No 9, pp. 1368-1382, Sept. 2000.

[4] J. Acero, C. Carretero, I. Lope, R. Alonso, Ó. Lucia, and J. M. Burdio, "Analysis of the Mutual Inductance of Planar-Lumped Inductive Power Transfer Systems," IEEE Transactions on Industrial Electronics, vol. 60, No. 1, pp. 410-420, January 2013.

[5] M. Derkaoui, Y. Benhadda, and A. Hamid, "Modeling and simulation of an integrated octagonal planar transformer for RF systems," SN Appl. Sci., vol. 2, no. 4, p. 656, Apr. 2020.

[6] F. Kahlouche, K. Youssouf, M. H. Bechir, S. Capraro, A. Siblini, J. P. Chatelon, C. Buttay, and J. J. Rousseau, "Fabrication and characterization of a planar interleaved micro-transformer with magnetic core," Microelectron. J., vol. 45, No 7, pp. 893-897, Jul. 2014.

[7] F. Tounsi, D. Flandre, L. Rufer, and L. A. Francis, "Performances Evaluation of On-Chip Large-Size-Tapped Transformer for MEMS Applications," IEEE Trans. Instrum. Meas., vol. 69, No 9, pp. 7051-7060, Sept. 2020.

[8] F. Tounsi, L. Rufer, B. Mezghani, M. Masmoudi and S. Mir, "Highly flexible membrane systems for micromachined microphones - modeling and simulation", 3rd International Conference on Signals Circuits and Systems (SCS), Medenine, Tunisia, pp. 1-6, Nov. 2009.

[9] O. El-Gharniti, E. Kerherve, and J.-B. Begueret, "Modeling and Characterization of On-Chip Transformers for Silicon RFIC," IEEE Trans. Microw. Theory Tech., vol. 55, No 4, pp. 607-615, Apr. 2007.

[10] Y. Cheng and Y. Shu, "A New Analytical Calculation of the Mutual Inductance of the Coaxial Spiral Rectangular Coils," IEEE Trans. Magn., vol. 50, No. 4, pp. 1–6, Apr. 2014.

[11] F. Tounsi, "Microphone électrodynamique MEMS en technologie CMOS: étude, modélisation et réalisation," Ph.D.Thesis, Institut National Polytechnique de Grenoble INPG, 2010.

[12] M. Damnjanovic, L. Zivanov, G. Radosavljevic, A. Maric and A. Menicanin, "Parameter extraction of ferrite transformers using S-parameters," 14th IEEE International Power Electronics and Motion Control Conference EPE-PEMC 2010, Ohrid, Macedonia, Sep. 2010.